Kidney failure in mice lacking the tetraspanin CD151

Norman Sachs,[1] Maaike Kreft,[1] Marius A. van den Bergh Weerman,[2] Andy J. Beynon,[3] Theo A. Peters,[3] Jan J. Weening,[2] and Arnoud Sonnenberg[1]

[1]Division of Cell Biology, The Netherlands Cancer Institute, 1066 CX Amsterdam, Netherlands
[2]Department of Pathology, Academic Medical Center, University of Amsterdam, 1105 AZ Amsterdam, Netherlands
[3]Department of Otorhinolaryngology, Radboud University Nijmegen Medical Center, 6500 HC Nijmegen, Netherlands

The tetraspanin CD151 is a cell-surface molecule known for its strong lateral interaction with the laminin-binding integrin α3β1. Patients with a nonsense mutation in *CD151* display end-stage kidney failure associated with regional skin blistering and sensorineural deafness, and mice lacking the integrin α3 subunit die neonatally because of severe abnormalities in the lung and kidney epithelia. We report the generation of *Cd151*-null mice that recapitulate the renal pathology of human patients, i.e., with age they develop massive proteinuria caused by focal glomerulosclerosis, disorganization of the glomerular basement membrane, and tubular cystic dilation. However, neither skin integrity nor hearing ability are impaired in the *Cd151*-null mice. Furthermore, we generated podocyte-specific conditional knockout mice for the integrin α3 subunit that show renal defects similar to those in the *Cd151* knockout mice. Our results support the hypothesis that CD151 plays a key role in strengthening α3β1-mediated adhesion in podocytes.

Introduction

Tetraspanins form a family of small proteins that are expressed in virtually all cell types and tissues (Boucheix and Rubinstein, 2001; Hemler, 2005). They consist of short intracellular termini, four transmembrane domains, and one small and one large extracellular loop that contain two highly conserved cysteine motifs. Tetraspanins oligomerize into tetraspanin-enriched microdomains, in which they associate with integrins, Ig superfamily members, growth factor receptors, and proteoglycans. Tetraspanin-enriched microdomains modulate diverse cellular activities, such as adhesion strengthening, migration, signal transduction, and proliferation (Hemler, 2005). The importance of proper tetraspanin function is demonstrated by several human diseases; distinct mutations in *A15* (*TSPAN7*) and *RDS* (*TSPAN22*) cause X-linked mental retardation and retinal dystrophy, respectively (Travis et al., 1989; Zemni et al., 2000). A nonsense mutation in *CD151* (*TSPAN24*) leads to end-stage hereditary nephropathy associated with pretibial epidermolysis bullosa and sensorineural deafness (Karamatic Crew et al., 2004).

CD151 is expressed in epithelia, endothelia, muscle cells, renal glomeruli, proximal and distal tubules, Schwann cells, platelets, and dendritic cells (Sincock et al., 1997; Sterk et al., 2002). Extensive biochemical studies have shown that CD151 is the primary tetraspanin associated with the laminin-binding integrins α3β1, α6β1, α6β4, and α7β1 (Sterk et al., 2000, 2002; Boucheix and Rubinstein, 2001; Hemler, 2005). The interaction of CD151 with α3β1 is particularly strong and occurs at high stoichiometry (Yauch et al., 1998).

Integrins are αβ heterodimeric cell surface proteins that dynamically link the extracellular matrix and/or adjacent cells to the intracellular cytoskeleton (van der Flier and Sonnenberg, 2001; Hynes, 2002). In epithelial cells, the integrins α3β1 and α6β4 are mainly present in the basolateral compartment, where they bind to the basement membrane component laminin-5. Although much more severe, the phenotypes associated with mutations in *Itga3*, *Itga6*, and *Itgb4* share features with the phenotype of patients with truncated CD151, indicating that the CD151–α3β1 and CD151–α6β4 heterotrimers are functionally important. Mice that lack the β4 subunit suffer from extensive detachment of the epidermis, and patients without functional α6β4 display junctional epidermolysis bullosa (Borradori and Sonnenberg, 1999; Uitto and Pulkkinen, 2001). Mice without α3 exhibit the mild skin blistering associated with ruptured basement membranes and die shortly after birth because of

N. Sachs and M. Kreft contributed equally to this paper.

Correspondence to Arnoud Sonnenberg: a.sonnenberg@nki.nl

Abbreviations used in this paper: ABR, auditory brainstem response; FP, foot process; GBM, glomerular basement membrane; GESD, glomerular epithelial slit diaphragm; pAb, polyclonal antibody.

The online version of this article contains supplemental material.

The Journal of Cell Biology, Vol. 175, No. 1, October 9, 2006 33–39
http://www.jcb.org/cgi/doi/10.1083/jcb.200603073

severe abnormalities in the epithelia of lung and kidney (Kreidberg et al., 1996; DiPersio et al. 1997).

In the renal glomerulus, podocytes are anchored to the glomerular basement membrane (GBM) via α3β1 and dystroglycans (Mundel and Shankland, 2002). The interdigitating foot processes (FPs) of podocytes are connected by glomerular epithelial slit diaphragms (GESDs) consisting of nephrin, podocin, P-cadherin, and other proteins, which are linked directly or indirectly to the cytoskeleton. Both disturbed podocyte–GBM anchoring and podocyte–podocyte interaction at the level of GESDs lead to the loss of FPs, a dysfunctional filtration barrier, and, ultimately, to glomerulosclerosis and renal failure (Pavenstädt et al., 2003).

We report the generation of knockout mice for *Cd151* that show severe renal failure caused by progressive abnormalities of the GBM, loss of podocyte FPs, glomerulosclerosis, and cystic tubular dilation. Furthermore, we show that mice with a targeted deletion of the α3 subunit in podocytes have a similar, although more severe, phenotype.

Results and discussion

Cd151-null mice were generated (Fig. S1, available at http://www.jcb.org/cgi/content/full/jcb.200603073/DC1), born at the expected Mendelian ratio (0.28 $^{(+/+)}$: 0.49 $^{(+/-)}$: 0.23 $^{(-/-)}$; $n = 86$), and appeared to be healthy and normal at first observation. However, urine analysis of *Cd151*$^{-/-}$ mice by SDS-PAGE revealed that all mice developed proteinuria before 3 wk of age, which is indicative of kidney dysfunction (Fig. 1 A). Both the onset and the degree of proteinuria were variable. Nevertheless, all knockout mice had to be killed before the age of 9 mo because of substantial loss of body weight. A quantitative immunoassay of urinary albumin showed high levels of this protein in *Cd151*$^{-/-}$ mice that increased with age and reached a plateau at 6 wk (3 mo follow up; unpublished data). In contrast, only traces of albumin were present in the urine of wild-type and *Cd151*$^{+/-}$ mice (Fig. 1, B and C). As expected, the severity of the renal pathology among *Cd151*$^{-/-}$ littermates also varied considerably (Fig. 2, A and B), and there were animals with mildly or severely affected kidneys in the same litter. Histological examination of the mildly affected kidneys showed focal glomerulosclerosis, and interstitial fibrosis and inflammation (Fig. 2, D and G). The GBM of some capillary loops was abnormally thick and formed extensive spikes (Fig. 2 J). EM revealed that the GBM was laminated and that FPs in contact with the abnormal GBM were effaced (Fig. 3, A–C). On the vascular side, the endothelium was swollen and fenestrations were occasionally lost (Fig. 3, B and C). Severely affected kidneys were contracted and their capsules granulated because of cortical degeneration (Fig. 2 B). Light microscopy showed extensive glomerulosclerosis in several stages, tuft adhesions to Bowman's capsule with extracapillary cell proliferation and fibrosis, and marked expansion of the mesangial matrix. Proximal tubuli were either dilated and contained PAS-positive protein casts or they displayed degeneration of varying severity (Fig. 2, E and H). Furthermore, we observed periglomerular fibrosis and focal interstitial inflammation in close proximity to interlobular blood vessels

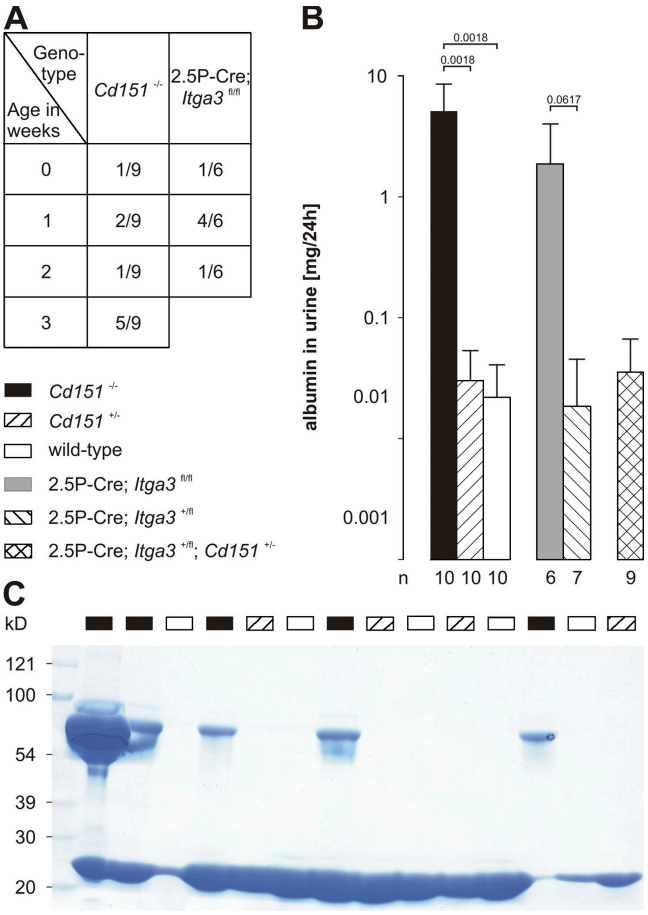

Figure 1. **Massive albuminuria in *Cd151*$^{-/-}$ and 2.5P-Cre; *Itga3*$^{fl/fl}$ mice.** (A) Age at which proteinuria was first detected by SDS-PAGE in *Cd151*$^{-/-}$ and 2.5P-Cre; *Itga3*$^{fl/fl}$ mice. (B) 24-h urinary albumin concentration in 6-wk-old mice as determined by competitive ELISA. Each bar represents the arithmetic mean ± the SD with P values, as determined by homoscedastic two-tailed *t* test, shown above it and the number of analyzed animals shown underneath. (C) Coomassie brilliant blue–stained gel showing the presence of albumin in the urine of *Cd151*$^{-/-}$ mice in a group of three litters (1 μl urine per lane; age, 6 wk).

(unpublished data). Silver staining showed the glomeruli to be segmentally or globally sclerosed with extensive deposits of basement membrane components (Fig. 2 K), an observation that could be confirmed by ultrastructural analysis (unpublished data). To investigate at what age GBM defects occur, we subjected kidneys of newborn and 1-wk-old *Cd151*$^{-/-}$ mice to EM. Although many capillary loops of newborn *Cd151*$^{-/-}$ mice already have a laminated GBM, it seems that spike formation does not occur until the mice are 1-wk-old (unpublished data). Together, these observations suggest that the mild abnormalities found in some of the mice represent early stages of the severe phenotype in the other mice. Tubular changes may be secondary to massive glomerular protein leakage, but may also reflect dysfunction of the tubules themselves.

To investigate whether the progressive GBM abnormalities are correlated with glomerular injury, we stained for tenascin-C and fibulin-2. Both proteins have been shown to be up-regulated in response to glomerular and vascular lesions (Assad et al., 1993; Wada et al., 2001). We observed an increased glomerular

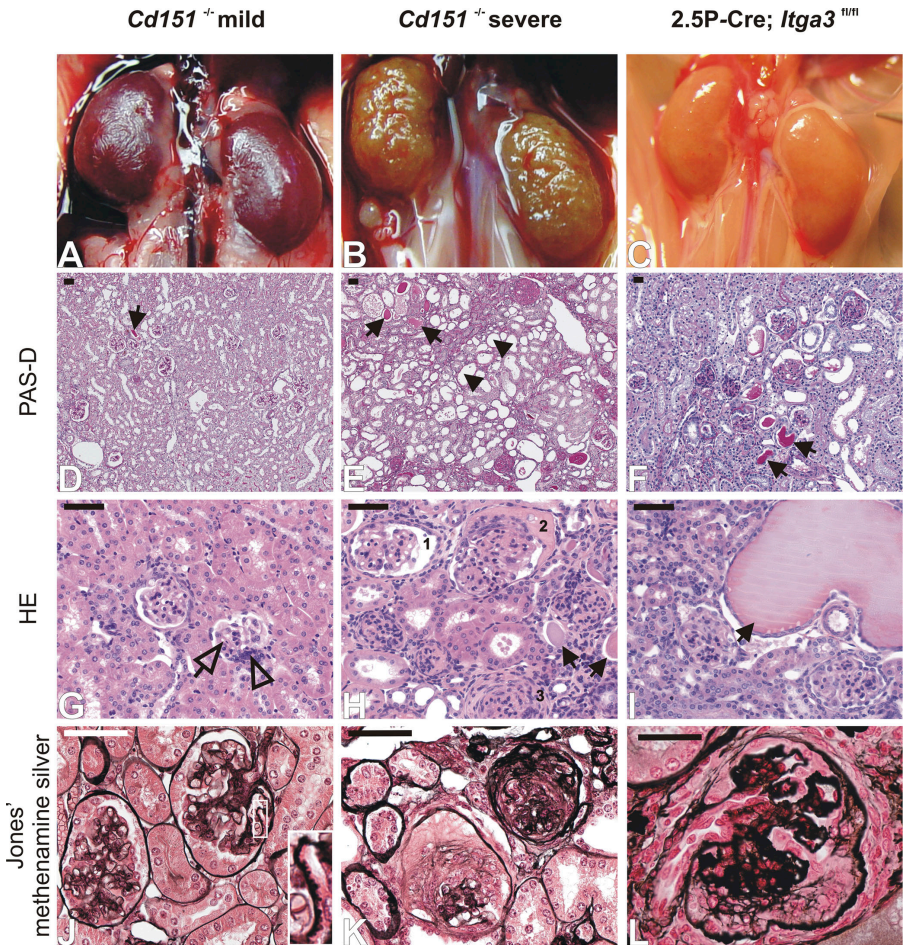

Figure 2. **Glomerular and tubular abnormalities in mutant mice.** Kidneys of *Cd151*$^{-/-}$ and 2.5P-Cre; *Itga3*$^{fl/fl}$ mice reveal mild (left column) and severe (middle and right columns) renal pathology. Although the mildly affected kidneys of a 3-mo-old *Cd151*$^{-/-}$ mouse show a relatively smooth and intact surface (A), histological examination reveals protein casts (D, arrow), inconspicuous interstitial fibrosis, mesangial hypercellularity (G, open arrowhead), and mild glomerular sclerosis (G, open arrow). The GBM shows partial thickening and spike formation (J, inset). Severe lesions of another 3-mo-old *Cd151*$^{-/-}$ mouse are characterized by a granular surface (B) caused by extensive glomerular collapsing sclerosis, periglomerular fibrosis, and focal interstitial inflammation and fibrosis (E, H, and K). The glomeruli show segmental (H, 1) and global (H, 2) attachment of glomerular tufts to Bowman's capsule, parietal epithelial crescents (H, 2), and hypercellularity, capillary collapse, and sclerosis (H, 3). Proximal tubuli show cystic dilation (E, arrowheads) and degeneration, as well as protein casts indicative of proteinuria (E and H, arrows). Silver staining indicates excessive GBM damage in some glomeruli (K). Severely affected kidneys of a 6-wk-old 2.5P-Cre; *Itga3*$^{fl/fl}$ mouse reveal prominent protein casts and some extremely dilated proximal tubuli (F and I, arrows). The glomeruli are partially sclerosed and show substantial damage of the GBM (L). Bars, 50 µm.

expression of tenascin-C in both mildly and severely affected kidneys, but fibulin-2 was up-regulated only in the latter (Fig. 4, A–C). Whereas fibulin-2 is important for the migration of smooth muscle cells, tenascin-C regulates migration of a variety of cell types, including fibroblasts (Hsia and Schwarzbauer, 2005; Strom et al., 2006). The finding that tenascin-C is already present in the early stages of the disease suggests that fibrosis precedes the pathology of the vasculature. Consistent with the ultrastructural finding that the GBM of *Cd151*$^{-/-}$ mice is thickened, staining for nidogen and laminin-10 revealed an abnormally strong presence of these GBM components in peripheral capillary loops and extracapillary spaces (Fig. 4, K–M and P–R). To exclude an arrest of the normal developmental switch from α1.α1.α2 (IV) collagen to the α3.α4.α5 (IV) and α5.α5.α6 (IV) collagen networks, as seen in the X-linked form of Alport's syndrome (Kalluri et al., 1997), we stained for all six chains of collagen IV. The results showed the mature collagen IV pattern to be present in all glomeruli (unpublished data). Only the α2 (IV) chain was strongly up-regulated in podocytes of the severely affected kidneys (Fig. 4 W). We also checked the integrity of the filtration barrier by staining for the GESD components podocin and nephrin (Fig. 4, P–R and U–W). Both proteins appeared to be down-regulated in the mildly affected kidneys, and are almost absent in the severely affected kidneys, demonstrating a complete loss of GESD architecture (Fig. 4, R and W). Together, these results support the hypothesis that in *Cd151*-null mice disorganization of the GBM precedes the effacement of FPs and the loss of GESDs. Patients with a nonsense mutation in *CD151* (Karamatic Crew et al., 2004) also have epidermolysis bullosa and deafness, but neither of these was observed in the *Cd151*$^{-/-}$ mice by histological and immunofluorescent analysis and measurements of auditory brainstem responses (ABR), respectively (Fig. S2, available at http://www.jcb.org/cgi/content/full/jcb.200603073/DC1).

The highly stoichiometric binding of CD151 to the α3β1 integrin, and the fact that mice lacking the α3 subunit show severe renal defects, led us to hypothesize that the absence of CD151–α3β1 complexes is responsible for the renal pathology seen in our *Cd151*-null mice. In *Itga3* knockout mice, glomerular capillary branching is impaired, leading to a decreased number of capillary loops. Furthermore, podocytes fail to form normal FPs and lose lateral cell junctions (Kreidberg et al., 1996). To study the deletion of *Itga3* after glomerular capillary branching, and to investigate possible similarities with the phenotype in our *Cd151*-null mice, we generated conditional *Itga3* knockout mice and crossed them with 2.5P-Cre mice that express the Cre recombinase under the control of the human podocin promoter (Moeller et al., 2003). As shown by immunofluorescence, α3 is, indeed, almost absent in the glomeruli of these 2.5P-Cre; *Itga3*$^{fl/fl}$ mice (Fig. 4, I and J), indicating that this integrin subunit is mainly expressed by differentiated podocytes. 2.5P-Cre; *Itga3*$^{fl/fl}$ mice show massive proteinuria starting within the first week of age (Fig. 1, A and B),

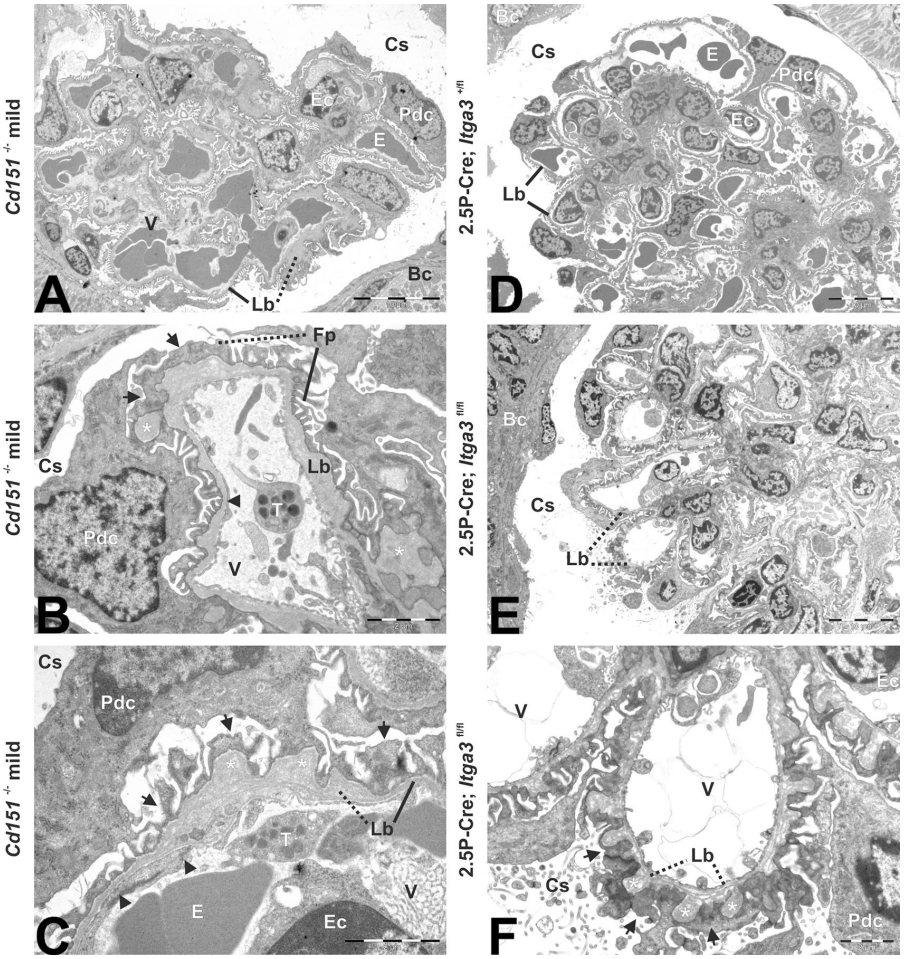

Figure 3. **Electron micrographs reveal GBM abnormalities and FP effacement in kidneys of mildly affected Cd151$^{-/-}$ and 2.5P-Cre; Itga3$^{fl/fl}$, but not 2.5P-Cre; Itga3$^{+/fl}$, mice.** (A) Glomeruli of *Cd151*$^{-/-}$ mice (3-mo-old) show abnormal capillary loops characterized by GBM thickening and loss of the regular pattern of podocyte FPs. (B) Peripheral glomerular capillary with a luminal thrombocyte and loss of fenestrations (arrowhead). The GBM is irregularly thickened and shows protrusions toward the capsular space (*). Podocyte FPs are partially lost (arrows). (C) Irregular GBM showing lamination, thickening, and protrusions (*). The endothelium is swollen and fenestrations are partially lost (arrowheads), as are podocyte FPs (arrows). Glomeruli of 6-wk-old 2.5P-Cre; *Itga3*$^{+/fl}$ mice do not show abnormalities (D), whereas all glomeruli of 2.5P-Cre; *Itga3*$^{fl/fl}$ mice exhibit severe structural changes (E and F). (E) Abnormally thickened GBM with protrusions throughout the glomerulus. (F) Podocyte FPs are completely lost (arrows) and GBM protrusions (*) are present along the entire length of the capillary loops. Solid lines point to normal structures (GBM and FPs), whereas dotted lines indicate abnormal thickening of the GBM and effacement of FPs. Bc, Bowman's capsule; Cs, capsular space; E, erythrocyte; Ec, endothelial cell; Fp, foot process; Lb, lamina basalis (GBM); Pdc, podocyte; T, thrombocyte; V, vascular lumen. Bars: (A, D, and E) 10 μm; (B, C, and F) 2 μm.

develop abdominal edema when 5–6-wk-old and, subsequently, have to be killed. Structurally, the milky, discolored kidneys contain partially sclerosed glomeruli with a disorganized GBM and prominent protein casts in dilated proximal tubuli (Fig. 2). EM revealed a complete effacement of podocyte FPs in newborns (unpublished data) and, in addition, widespread lamination and protrusions of the GBM in 6-wk-old mice (Fig. 3, E and F). Immunofluorescence showed changes similar to those in *Cd151*$^{-/-}$ mice, i.e., up-regulation of tenascin-C and fibulin, strong staining of the GBM components nidogen and laminin-10, and down-regulation of the GESD proteins podocin and nephrin (Fig. 4). Notably, sclerosis of the glomeruli, up-regulation of the collagen α2 (IV) chain, and down-regulation of podocin and nephrin is much less prominent in the 2.5P-Cre; *Itga3*$^{fl/fl}$ mice than in the *Cd151* knockout mice. 2.5P-Cre; *Itga3*$^{+/fl}$ mice do not develop structural or functional renal abnormalities (Fig. 1 A, Fig. 3 D, and Fig. 4); neither do 6-wk-old compound heterozygotes (2.5P-Cre; *Itga3*$^{+/fl}$; *Cd151*$^{+/-}$), which may suggest that a simultaneous reduction of α3 and CD151 does not result in renal defects (Fig. 1 C). However, we cannot prove that the expression of these proteins is actually reduced in the compound heterozygotes, nor can we exclude that renal pathology develops upon aging.

Because *Cd151*-null mice can form normal GBMs with a regular FP pattern (Fig. 3 A) and expression of both α3 and α6 in the glomeruli and tubules appeared to be normal (Fig. 4, F–H), we suggest that the function of α3 in development is not affected by the absence of CD151. Instead, we propose that reduced integrin α3β1-mediated adhesion is the main cause of the phenotype observed in our *Cd151*$^{-/-}$ mice. The filtration of plasma exerts considerable mechanical stress on the filtration barrier. Podocyte FPs, thus, have to withstand substantial mechanical forces. Indeed, CD151 appears to be involved in adhesion strengthening because adhesions mediated by CD151–α6β1 complexes tolerate stronger mechanical forces than those mediated by α6β1 alone (Lammerding et al., 2003). A similar effect has been suggested for CD151–α3β1 complexes (Nishiuchi et al., 2005). Thus, FPs without CD151 might not be able to withstand prolonged transcapillary pressure, a phenomenon that is also responsible for the renal manifestations in the Alport's syndrome after several years of life in patients with an abnormal GBM caused by collagen type IV mutations (Kalluri et al., 1997). Epithelial cells may become partially detached, leading to a compensatory production of new basement membrane components. As a result, the GBM thickens and spikes are formed, as has also been described in membranous nephropathy (Minto et al., 1998). Correct reassembly of basement membranes upon injury is impaired in the skin of *Cd151*-null mice (Cowin et al., 2006). If the absence of CD151 is similarly important for GBM repair, this vicious circle would indeed result in glomerular malfunction. As shown by ultrastructural and immunofluorescent analysis,

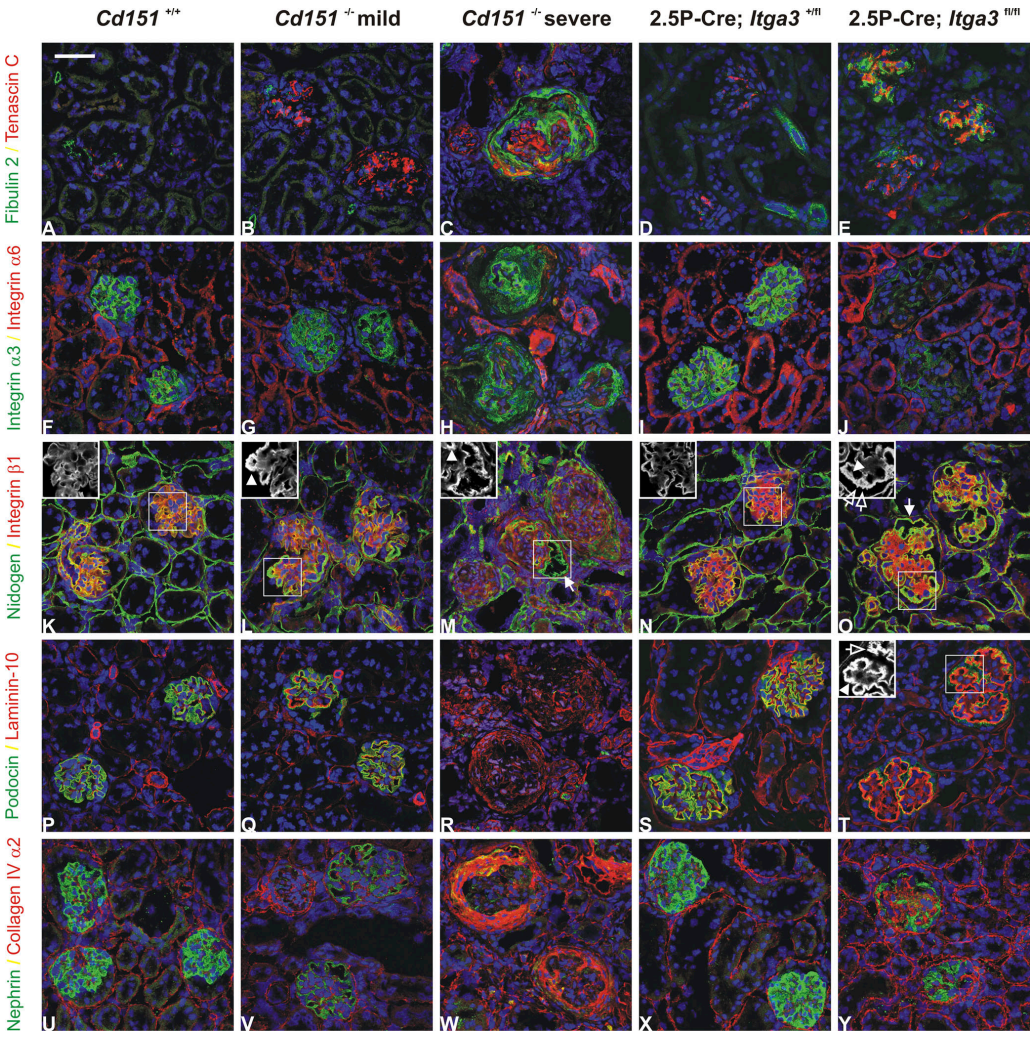

Figure 4. **Histological analysis of *Cd151*$^{-/-}$ and 2.5P-Cre; *Itga3*$^{fl/fl}$ mice.** Immunofluorescence analysis of kidneys from 3-mo-old wild-type (left column), mildly affected, and severely affected *Cd151*$^{-/-}$ (second and third column), and 6-wk-old 2.5P-Cre; *Itga3*$^{+/fl}$ and 2.5P-Cre; *Itga3*$^{fl/fl}$ mice (columns four and five). The respective proteins are shown in green and red, yielding yellow upon colocalization. Nuclei are counterstained with TOPRO (blue). (A–C) Up-regulation of tenascin-C in the mildly affected, and of fibulin-2 in the severely affected, *Cd151*$^{-/-}$ glomeruli. (D and E) 2.5P-Cre; *Itga3*$^{+/fl}$ glomeruli show little presence of tenascin-C, whereas both tenascin-C and fibulin-2 are present in glomeruli of 2.5P-Cre; *Itga3*$^{fl/fl}$ mice. (F–I) Integrin α3 and α6 are localized in glomeruli and tubules, respectively, in both wild-type and mildly affected *Cd151*$^{-/-}$ kidneys, as well as in the kidneys of 2.5P-Cre; *Itga3*$^{+/fl}$ mice. (J) Hardly any α3 is present in the glomeruli of 2.5P-Cre; *Itga3*$^{fl/fl}$ mice, whereas α6 is normally distributed in the tubules. (K and N) Staining of nidogen shows regular GBMs in both wild-type and 2.5P-Cre; *Itga3*$^{+/fl}$ mice. (L and M) Unusually strong nidogen staining of the GBM of peripheral capillary loops in both mildly and severely affected *Cd151*$^{-/-}$ kidneys (arrowheads). Note the extracapillary accumulation of nidogen (arrow) and massive capillary collapse (β1 staining) in the severely affected kidneys. (O) Nidogen also accumulates in the capsular space of 2.5P-Cre; *Itga3*$^{fl/fl}$ mice (arrow). Glomeruli are not collapsed, but show an abnormally thick GBM (arrowhead) with protrusions (open arrow). (P–T) Podocin is present along the glomerular tuft in wild-type, mildly affected *Cd151*$^{-/-}$, and 2.5P-Cre; *Itga3*$^{+/fl}$ mice, but absent in severely affected *Cd151*$^{-/-}$ and 2.5P-Cre; *Itga3*$^{fl/fl}$ mice. Staining of laminin-10 shows sclerosed glomeruli in *Cd151*$^{-/-}$ mice (R) and GBM thickening (arrowhead) with protrusions (open arrow) in 2.5P-Cre; *Itga3*$^{fl/fl}$ mice (T). (U–W) Nephrin is lost in some glomeruli of mildly affected *Cd151*$^{-/-}$ mice, but in all glomeruli of the severely affected *Cd151*$^{-/-}$ mice. There is massive up-regulation of the collagen α2 (IV) in the severe *Cd151*$^{-/-}$ phenotype (W) which is further characterized by hypercellularity in both the interstitium and glomeruli (C, H, M, R, and W; blue channel). (X and Y) Nephrin is also reduced in 2.5P-Cre; *Itga3*$^{fl/fl}$ mice as compared with the conditional heterozygote, whereas the collagen α2 (IV) is hardly up-regulated. Insets K–O, green channel (nidogen); Inset T, red channel (laminin-10). Bar, 50 μm.

glomerulosclerosis precedes the loss of GESD components, leading to the aforementioned renal pathology.

The assumption that CD151 is important for maintaining glomerular architecture upon mechanical stress is in accordance with the observation that glomeruli develop normally and that abnormalities only occur after several weeks or months. Furthermore, it explains differences in the rate of progression among littermates, as the degree of intraglomerular hydrostatic pressure depends on several genetic and epigenetic factors. Differences in genetic background might also explain why *Cd151*-null mice that have been previously described did not show renal failure as observed in our mice (Wright et al., 2004). In conclusion, we show that the renal manifestations in our mice lacking CD151 are similar to those in patients with a mutated *CD151*. Our data support in vitro studies pointing to a role of CD151 in adhesion strengthening, thus, suggesting that CD151–α3β1 complexes have an essential function in vivo.

Materials and methods

Urine analysis
Urine from mice younger than 3-wk-old were collected by applying gentle dorsal pressure to the caudal area of the animal. Older mice were placed in metabolic cages for 24 h. Samples were either analyzed by SDS-PAGE, followed by Coomassie Brilliant blue staining, or by competitive ELISA using the Albuwell M kit that was obtained from Exocell.

Histological analysis
Sections of kidneys were prepared, fixed for 1 d in EAF (ethanol, acetic acid, and formaldehyde), and stained with PAS-D, HE, or Jones' methenamine silver. Images were taken with PL APO objectives (10×/0.25 NA, 40×/0.95 NA, and 63×/1.4 NA oil; Carl Zeiss MicroImaging, Inc.) on an Axiovert S100/AxioCam HR color system using AxioVision 4 software (Carl Zeiss MicroImaging, Inc.).

Ultrastructural analysis
After fixation in Karnovsky buffer for 48 h, the material was post-fixed with 1% osmiumtetroxide, the tissue samples were block-stained with 1% uranyl acetate, dehydrated in dimethoxypropane, and embedded in epoxyresin LX-112. LM sections were stained with toluidine blue. EM sections were stained with tannic acid, uranyl acetate, and lead citrate, and then examined using a transmission electron microscope (Philips CM10; FEI). Images were acquired using a digital transmission EM camera (Morada 10–12; Soft Imaging System) using Research Assistant software (RvC).

Antibodies
Rat mAbs used in this study were 4G6 against laminin-10 (provided by L. Sorokin, University of Münster, Münster, Germany), GoH3 against α6, MB1.2 against β1 (a gift from B.M. Chan, University of Western Ontario, London, Canada), LAT-2 against tenascin-C (van der Flier et al., 1997), and 346-11A against β4 (Abcam). Y. Sado (Shigei Medical Research Institute, Yamada, Japan) provided the rat mAbs H11, H22, H31, RH42, M54, and B66 against the mouse collagen IV chains α1, α2, α3, α4, α5, and α6, respectively. Rabbit polyclonal antibodies (pAbs) directed against mouse nidogen and mouse fibulin-2 were generous gifts from T. Sasaki (Max Planck Institute for Biochemistry, München, Germany); pAbs against nephrin and podocin were from H. Holthöfer (University of Helsinki, Helsinki, Finland), and C. Antignac (Cochin Biomedical Research Institute, Paris, France). The pAbs against keratin 1 and 14 were purchased from BabCO. Immunization of New Zealand rabbits with the cytoplasmic tail of human α3A fused to GST and the peptide CKENLKDTMVKRYHQSGHEGVSSAVDKLQQEFH coupled to KLH (Pierce Chemical Co.) yielded pAbs 141742 against α3A and 140190 against CD151, respectively. Texas red– and FITC-conjugated secondary antibodies were purchased from Invitrogen.

Immunofluorescence microscopy
Tissues from adult mice were collected and embedded in cryoprotectant (Tissue-Tek O.C.T.; Sakura Finetek Europe). Cryosections were prepared, fixed in ice-cold acetone, blocked with 2% BSA in PBS, and incubated for 45 min with primary antibodies undiluted (LAT-2, GoH3, MB1.2, 4G6) or diluted 1:2 (H22), 1:50 (346-11A), 1:100 (anti–fibulin-2, anto-podocin, anti-nephrin, and 141742), 1:250 (anti-nidogen), and 1:300 (anti-keratin 1 and 14), followed by incubation with secondary antibodies diluted 1:200 for 45 min. Samples were analyzed at 37°C using a 63×/1.4 HCX PL APO CS objective on a TCS SP2 AOBS confocal microscope (both from Leica). Images were acquired using LCS 2.61 (Leica) and processed using CorelDRAW Graphics Suite 12 (Corel).

Online supplemental material
Fig. S1 shows the targeting strategy and molecular analysis of recombinant embryonic stem cells and *Cd151* knockout mice. Fig. S2 shows the histology and immunofluorescence analysis of keratins 1 and 14 on back skin samples from wild-type and $Cd151^{-/-}$ mice, as well as auditory hearing thresholds of wild-type, $Cd151^{+/-}$, and $Cd151^{-/-}$ mice upon click and tone burst stimuli, as determined by ABR measurements. The Supplemental materials and methods describes the generation of transgenic mice, immunoblotting, and ABR measurements. Online supplemental material is available at http://www.jcb.org/cgi/content/full/jcb.200603073/DC1.

We are grateful to Dr. L.B. Holzman for generously providing the 2.5P-Cre transgenic mice, and to Drs. C. Antignac, A. Bradley, B. Chan, B. Lane, H. Holthofer, Y. Sado, and T. Sasaki for providing reagents. We would like to thank Dr. K. Wilhelmsen and I. Kuikman for the generation of antibodies against CD151 and the integrin α3 subunit.

This work was supported by grants from the Dutch Cancer Society and the Netherlands Kidney Foundation.

Submitted: 16 March 2006
Accepted: 5 September 2006

References

Assad, L., M.M. Schwartz, I. Virtanen, and V.E. Gould. 1993. Immunolocalization of tenascin and cellular fibronectins in diverse glomerulopathies. *Virchows Arch. B Cell Pathol. Incl. Mol. Pathol.* 63:307–316.

Borradori, L., and A. Sonnenberg. 1999. Structure and function of hemidesmosomes: more than simple adhesion complexes. *J. Invest. Dermatol.* 112:411–418.

Boucheix, C., and E. Rubinstein. 2001. Tetraspanins. *Cell. Mol. Life Sci.* 58:1189–1205.

Cowin, A.J., D. Adams, S.M. Geary, M.D. Wright, J.C. Jones, and L.K. Ashman. 2006. Wound healing is defective in mice lacking tetraspanin CD151. *J. Invest. Dermatol.* 126:680–689.

DiPersio, C.M., K.M. Hodivala-Dilke, R. Jaenisch, J.A. Kreidberg, and R.O. Hynes. 1997. α3β1 integrin is required for normal development of the epidermal basement membrane. *J. Cell Biol.* 137:729–742.

Hemler, M.E. 2005. Tetraspanin functions and associated microdomains. *Nat. Rev. Mol. Cell Biol.* 6:801–811.

Hsia, H.C., and J.E. Schwarzbauer. 2005. Meet the tenascins: multifunctional and mysterious. *J. Biol. Chem.* 280:26641–26644.

Hynes, R.O. 2002. Integrins: bidirectional, allosteric signaling machines. *Cell.* 110:673–687.

Kalluri, R., C.F. Shield, P. Todd, B.G. Hudson, and E.G. Neilson. 1997. Isoform switching of type IV collagen is developmentally arrested in X-linked Alport syndrome leading to increased susceptibility of renal basement membranes to endoproteolysis. *J. Clin. Invest.* 99:2470–2478.

Karamatic Crew, V., N. Burton, A. Kagan, C.A. Green, C. Levene, F. Flinter, R.L. Brady, G. Daniels, and D.J. Anstee. 2004. CD151, the first member of the tetraspanin (TM4) superfamily detected on erythrocytes, is essential for the correct assembly of human basement membranes in kidney and skin. *Blood*. 104:2217–2223.

Kreidberg, J.A., M.J. Donovan, S.L. Goldstein, H. Rennke, K. Shepherd, R.C. Jones, and R. Jaenisch. 1996. α3β1 integrin has a crucial role in kidney and lung organogenesis. *Development*. 122:3537–3547.

Lammerding, J., A.R. Kazarov, H. Huang, R.T. Lee, and M.E. Hemler. 2003. Tetraspanin CD151 regulates α6β1 integrin adhesion strengthening. *Proc. Natl. Acad. Sci. USA*. 100:7616–7621.

Minto, A.W., R. Kalluri, M. Togawa, E.C. Bergijk, P.D. Killen, and D.J. Salant. 1998. Augmented expression of glomerular basement membrane specific type IV collagen isoforms (α3-α5) in experimental membranous nephropathy. *Proc. Assoc. Am. Physicians*. 110:207–217.

Moeller, M.J., S.K. Sanden, A. Soofi, R.C. Wiggins, and L.B. Holzman. 2003. Podocyte-specific expression of Cre recombinase in transgenic mice. *Genesis*. 35:39–42.

Mundel, P., and S.J. Shankland. 2002. Podocyte biology and response to injury. *J. Am. Soc. Nephrol.* 13:3005–3015.

Nishiuchi, R., N. Sanzen, S. Nada, Y. Sumida, Y. Wada, M. Okada, J. Takagi, H. Hasegawa, and K. Sekiguchi. 2005. Potentiation of the ligand-binding activity of integrin α3β1 via association with tetraspanin CD151. *Proc. Natl. Acad. Sci. USA*. 102:1939–1944.

Pavenstädt, H., W. Kriz, and M. Kretzler. 2003. Cell biology of the glomerular podocyte. *Physiol. Rev.* 83:253–307.

Sincock, P.M., G. Mayrhofer, and L.K. Ashman. 1997. Localization of the transmembrane 4 superfamily (TM4SF) member PETA-3 (CD151) in normal human tissues: comparison with CD9, CD63, and α5β1 integrin. *J. Histochem. Cytochem.* 45:515–525.

Sterk, L.M., C.A. Geuijen, L.C. Oomen, J. Calafat, H. Janssen, and A. Sonnenberg. 2000. The tetraspan molecule CD151, a novel constituent of hemidesmosomes, associates with the integrin α6β4 and may regulate the spatial organization of hemidesmosomes. *J. Cell Biol.* 149:969–982.

Sterk, L.M., C.A. Geuijen, J.G. van den Berg, N. Claessen, J.J. Weening, and A. Sonnenberg. 2002. Association of the tetraspanin CD151 with the laminin-binding integrins α3β1, α6β1, α6β4 and α7β1 in cells in culture and in vivo. *J. Cell Sci.* 115:1161–1173.

Strom, A., A.I. Olin, A. Aspberg, and A. Hultgardh-Nilsson. 2006. Fibulin-2 is present in murine vascular lesions and is important for smooth muscle cell migration. *Cardiovasc. Res.* 69:755–763.

Travis, G.H., M.B. Brennan, P.E. Danielson, C.A. Kozak, and J.G. Sutcliffe. 1989. Identification of a photoreceptor-specific mRNA encoded by

the gene responsible for retinal degeneration slow (rds). *Nature*. 338:70–73.

Uitto, J., and L. Pulkkinen. 2001. Molecular genetics of heritable blistering disorders. *Arch. Dermatol.* 137:1458–1461.

van der Flier, A., and A. Sonnenberg. 2001. Function and interactions of integrins. *Cell Tissue Res.* 305:285–298.

van der Flier, A., A.C. Gaspar, S. Thorsteinsdóttir, C. Baudoin, E. Groeneveld, C.L. Mummery, and A. Sonnenberg. 1997. Spatial and temporal expression of the β1D integrin during mouse development. *Dev. Dyn.* 210:472–486.

Wada, J., H. Zhang, Y. Tsuchiyama, K. Hiragushi, K. Hida, K. Shikata, Y.S. Kanwar, and H. Makino. 2001. Gene expression profile in streptozotocin-induced diabetic mice kidneys undergoing glomerulosclerosis. *Kidney Int.* 59:1363–1373.

Wright, M.D., S.M. Geary, S. Fitter, G.W. Moseley, L.M. Lau, K.C. Sheng, V. Apostolopoulos, E.G. Stanley, D.E. Jackson, and L.K. Ashman. 2004. Characterization of mice lacking the tetraspanin superfamily member CD151. *Mol. Cell. Biol.* 24:5978–5988.

Yauch, R.L., F. Berditchevski, M.B. Harler, J. Reichner, and M.E. Hemler. 1998. Highly stoichiometric, stable, and specific association of integrin α3β1 with CD151 provides a major link to phosphatidylinositol 4-kinase, and may regulate cell migration. *Mol. Biol. Cell*. 9:2751–2765.

Zemni, R., T. Bienvenu, M.C. Vinet, A. Sefiani, A. Carrie, P. Billuart, N. McDonell, P. Couvert, F. Francis, P. Chafey, et al. 2000. A new gene involved in X-linked mental retardation identified by analysis of an X;2 balanced translocation. *Nat. Genet.* 24:167–170.